JOURNAL OF VIROLOGY, June 1996, p. 3734–3740
0022-538X/96/$04.00+0

Vol. 70, No. 6

Measles Virus Infection of Thymic Epithelium in the SCID-hu Mouse Leads to Thymocyte Apoptosis

PAUL G. AUWAERTER,[1] HIDETO KANESHIMA,[2] JOSEPH M. McCUNE,[2]† GORDON WIEGAND,[3] AND DIANE E. GRIFFIN[1,4,5]*

Division of Infectious Diseases[1] and Division of Rheumatology,[3] Department of Medicine and Department of Neurology,[4] Johns Hopkins University School of Medicine, and Department of Molecular Microbiology and Immunology, Johns Hopkins University School of Public Health,[5] Baltimore, Maryland 21287, and SyStemix, Palo Alto, California 94304[2]

Received 30 November 1995/Accepted 21 February 1996

Mortality from measles is caused mostly by secondary infections associated with the depression of cellular immunity. The mechanism of immune suppression and the role of virus strain differences on the immune system are incompletely understood. SCID-hu mice were used to determine the effects of virulent, wild-type (Chicago-1) and avirulent, vaccine (Moraten) strains of measles virus (MV) on the human thymus in vivo. Chicago-1 replicated rapidly, with a 100-fold decrease in numbers of thymocytes, whereas Moraten replicated slowly, without significant thymocyte death. Productive MV infection occurred not in thymocytes but in thymic epithelial and myelomonocytic cells. Wild-type MV infection of thymic stromata leads to induction of thymocyte apoptosis and may contribute to a long-term alteration of immune responses. The extent of thymic disruption reflects the virulence of the virus, and therefore the SCID-hu mouse may serve as the first small animal model for the study of MV pathogenesis.

Measles virus (MV) infection remains a significant cause of morbidity and mortality accounting for more than 1 million deaths annually, especially among infants and young children in developing countries (19). Most deaths are due to secondary infections which appear to be a consequence of MV-induced immune suppression (7, 28). The suppression of delayed-type hypersensitivity reactions was first described in 1908 by von Pirquet, who noted the disappearance of tuberculin skin test reactions during and after recovery from measles (49). This may be due in part to a skew toward type 2 T-cell responses which favor antibody production while suppressing type 1 cell-mediated responses (50, 51). Although malnutrition and limited access to medical care may be contributing factors, the severity of measles in the young remains without clear explanation (6, 41). MV infects the thymus during human and primate illness (23, 30, 38, 40, 52), and we postulated that this may contribute to immune suppression, particularly in infants. Thymic cellular disruption and necrosis have been reported following measles-related deaths, but these findings have been difficult to relate directly to virus infection (10–12).

Strains of MV differ in virulence, but the basis for attenuation of the vaccine strains is unknown. Since MV is a human pathogen, studies of pathogenesis and the determinants of virulence have been hampered by the lack of a suitable animal model. Rodents can be successfully infected with neuroadapted strains, but these nervous system infections bear little resemblance to typical human measles (25). Primates can be infected but display clinical disease infrequently, and extensive monkey studies of measles pathogenesis are impractical (47).

Immunodeficient SCID mice with coimplants of human fetal thymus and liver cells (Thy-Liv) placed under the murine kidney capsule have been useful for the study of certain aspects of human immunodeficiency virus (HIV) (2, 9, 27, 33, 45), cytomegalovirus (CMV) (29), and varicella-zoster virus (31) infection. These human coimplants develop into phenotypically normal and functionally competent thymuses with complete T-cell lymphopoietic lineages (24, 26). SCID-hu mice with Thy-Liv implants were used to determine the effects of a recent U.S. wild-type isolate (Chicago-1 [Chi-1]) and an avirulent, attenuated-vaccine strain (Moraten [Mor]) of MV on thymus cells in vivo.

MATERIALS AND METHODS

MV infection of SCID-hu mice. SCID-hu mice with Thy-Liv implants were constructed as previously described (34). All animals were cared for in accordance with guidelines set by animal care committees of Johns Hopkins University School of Medicine and of SyStemix. Animals were anesthetized with ketamine (200 μg administered intraperitoneally) and methoxyflurane (3%) for procedures associated with implantation and viral inoculation. Vero cell-derived viral stocks (Chi-1 and Mor) or mock-infected Vero cell supernatants (10^3 PFU in final volumes of 30 to 50 μl per implant) were injected intrathymically with a 30-gauge needle. Experimental results are a compilation of three experiments. For all time points, three animals were used per virus with the exception of day 21 with Mor, for which five animals were used. One mock-infected animal was assessed per time point. Chi-1 and Mor strains of MV were kindly provided by William Bellini and Paul Rota, Centers for Disease Control and Prevention. The Bilthoven strain was generously provided by A. D. M. E. Osterhaus, Erasmus University, Rotterdam, and propagated on phytohemagglutinin (2.5 μg/ml)-stimulated human cord blood mononuclear cells.

Assessment of viral titer and thymocyte cell number. At intervals, Thy-Liv implants were harvested and divided into thirds. One-third was completely homogenized, frozen, and thawed, with the resultant supernatant titered onto Vero cell monolayers as previously described (1). Another third was gently disrupted to release thymocytes into ice-cold phosphate-buffered saline (PBS). Portions of the cells were stained with 0.1% trypan blue, and dye-excluding cells were counted with a hemocytometer. The remaining cells of this lot were then used for flow cytometry. The remaining third of the implant was used for histological studies.

Thymic histology and immunofluorescence studies. Thymic implants were either fixed in 4% paraformaldehyde prior to paraffin embedding or freshly frozen. Paraffin-embedded specimens were stained with hematoxylin and eosin. Frozen tissues were embedded in Tissue-Tek OCT (Miles, Elkhart, Ind.) and snap frozen in an isopentane bath. Air-dried sections (5 to 6 μm) were fixed and permeabilized with ice-cold acetone. For double-immunofluorescent staining, tissues were incubated with murine monoclonal antibodies directed against MV hemagglutinin (HA) (either fluorescein isothiocyanate [FITC]-MV HA [F182r; Accurate, Westbury, N.Y.] or unconjugated MV HA [8905; Chemicon, Temacula, Calif.]) or MV nucleoprotein (N-25, kindly provided by F. Wild, Lyon,

* Corresponding author. Mailing address: Meyer 6-181, 600 N. Wolfe St., Baltimore, MD 21287. Phone: (410) 955-3726. Fax: (410) 955-0672. Electronic mail address: dgriffin@welchlink.welch.jhu.edu.

† Present address: Gladstone Institute of Virology and Immunology, University of California, San Francisco, CA 94141.

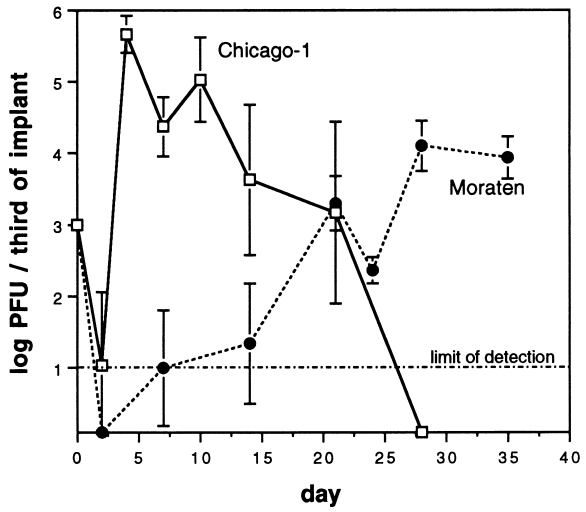

FIG. 1. Growth of two strains of MV in Thy-Liv implants. SCID-hu mice were infected by direct inoculation of the Thy-Liv grafts with 10^3 PFU of either a wild-type strain (Chi-1) or an attenuated strain (Mor) of MV. Thy-Liv implants were harvested from three or five mice from each group at intervals over 35 days. Viral titers were assessed from cell-free homogenates taken from one-third of the implant. Data are plotted as geometric means ± standard errors of the means.

France) and epithelial marker anti-keratin (AE1/AE3; Boehringer Mannheim, Indianapolis, Ind.), myelomonocytic marker FITC-CD15 (Leu-M1; Becton Dickinson, Mountain View, Calif.), or thymocyte markers phycoerythrin-CD1a (Coulter, Hialeah, Florida), FITC-CD2, FITC-CD4, FITC-CD8, or FITC-CD45 (Becton Dickinson). Tissues were washed extensively in PBS containing normal mouse serum or normal goat serum prior to antibody incubation. Secondary antibodies used were either a Texas Red-conjugated goat anti-mouse immunoglobulin G (Caltag, South San Francisco, Calif.) or FITC-conjugated goat anti-mouse immunoglobulin G (Immunotech, Westbrook, Mass.).

Flow cytometry. Suspended thymocytes were washed with cold PBS with 2% fetal bovine serum (GIBCO, Grand Island, N.Y.). FITC-Leu 2a (CD8) and phycoerythrin-Leu 3a (CD4) were used as described by the manufacturer (Becton Dickinson). Thymocytes were simultaneously stained with PerCP-Leu 4 (CD3) (Becton Dickinson). A live gate based on forward and side scatter was used to exclude dead cells and doublets with a single-laser FACScanner (Becton Dickinson). Separate groups of thymocytes were also stained with FITC-CD2, CD46 (J4-48; Immunotech) with goat anti-mouse FITC-immunoglobulin G (Immunotech), and propidium iodide (Molecular Probes, Eugene, Oreg.), which was added to a final concentration of 1 μg/ml 10 min prior to analysis. Statistical analysis was determined with StatView 4.01 software (Abacus Concepts, Berkeley, Calif.) by an unpaired two-tailed *t* test.

Determination of thymocyte apoptosis. An adapted terminal deoxynucleotidyl transferase-mediated dUTP nicked-end labeling (TUNEL) assay (16) used paraffin-embedded specimens that were subsequently deparaffinized, hydrated through a series of graded alcohols, and permeabilized with proteinase K (10 μg/ml). After dehydration, end labeling was achieved with terminal deoxynucleotidyl transferase (0.75 U/μl) and digoxigenin-labeled dUTP (0.25 nM) (Boehringer Mannheim) in 30 mM Tris-HCl (pH 7.2)–140 mM Na cacodylate–1 mM cobalt chloride for 1 h at 37°C. Slides were washed in 2× SSC (1× SSC is 0.15 M NaCl, 10 mM NaH_2PO_4, and 1 mM EDTA [pH 7.7]) and PBS before incubation in alkalinized buffers including 2% normal sheep serum prior to incubation with sheep anti-digoxigenin antibody (Boehringer Mannheim). Following two more washes, slides were visualized with nitroblue tetrazolium and an alkaline phosphatase solution (Boehringer Mannheim) with levamisole added to block endogenous phosphatases. Following a sufficient reaction time, slides were washed, dehydrated, and mounted.

RESULTS

Replication of MV within Thy-Liv implants. Thy-Liv implants were infected by direct intrathymic inoculation with 10^3 PFU of either Chi-1 or Mor. All SCID-hu mice remained without clinical signs of illness during this study. Peak viral titers (Fig. 1) were reached with Chi-1 4 to 10 days after infection (mean, $10^{5.0–5.7}$ PFU per one-third of implant), and this virus could no longer be recovered at 28 days. Mor remained below limits of detection until 14 days after infection and then rose in titer until 28 to 35 days ($10^{3.9–4.1}$ PFU per one-third of implant). Wild-type and attenuated MV strains have been reported to replicate similarly in vitro but with different plaque morphologies (1). Studies of the kinetics of replication of Chi-1 and Mor in Vero cells differed in that Chi-1 produced new virus 2 days earlier than Mor, but both reached similar peak titers (10^6 PFU/ml) by days 2 and 5, respectively (data not shown). The extensive differences in replication rates between Mor and Chi-1 in Thy-Liv implants appear to reflect unique in vivo biologic properties of these strains of MV.

MV strain-dependent effects on thymic microenvironment. Replication of Chi-1 was associated with a 100-fold decrease in the number of viable thymocytes recoverable per implant compared with that of the mock-infected controls (Fig. 2). Despite the production of slowly increasing amounts of Mor, thymocyte numbers remained unchanged and similar to those of controls. Thymuses infected with Chi-1 were virtually devoid of normal thymocytes by day 14 (Fig. 3C), whereas those infected with Mor (Fig. 3B) maintained cellularity and architecture similar to those of uninfected controls (Fig. 3A). Despite a rising viral titer at day 35, Mor-infected implants remained relatively undisturbed histologically (Fig. 3D). Higher magnification (data not shown) revealed marked thymocyte pyknosis and nuclear condensation in implants infected with Chi-1 starting at day 4. Only occasional pyknotic cells were seen in Mor-infected implants, and no such cells were seen in mock-infected controls. There also was evidence of extensive thymic stromal cell vacuolization and nuclear fragmentation in Chi-1-infected implants.

To determine whether there was a preferential loss of specific thymocyte subpopulations, MV-infected Thy-Liv implants were examined by flow cytometry. Declines in cell numbers were most marked in the $CD4^+$ $CD8^+$ population (Fig. 4) in Chi-1-infected implants with a concomitant relative rise in the percentage of cells in the $CD4^{-/lo}$ $CD8^{-/lo}$ population. The rise in this latter thymocyte population following Chi-1 infection (Table 1) correlated with a loss of the thymocyte marker

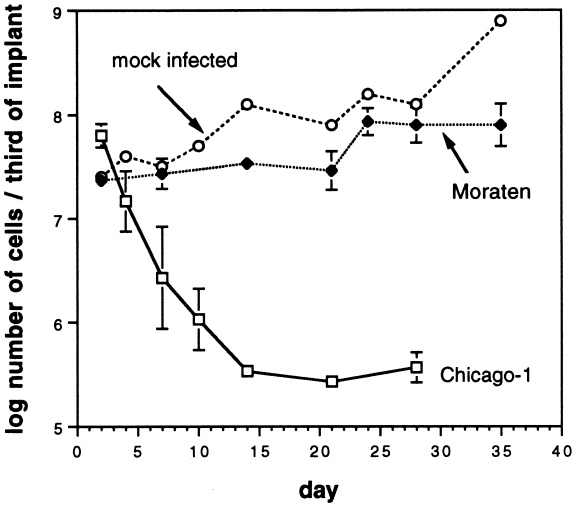

FIG. 2. Effects of infection with two strains of MV on thymocyte numbers in SCID-hu Thy-Liv implants. Data represent total viable thymocyte numbers obtained from one-third of each implant, based on cells excluding the trypan blue stain (0.1%).

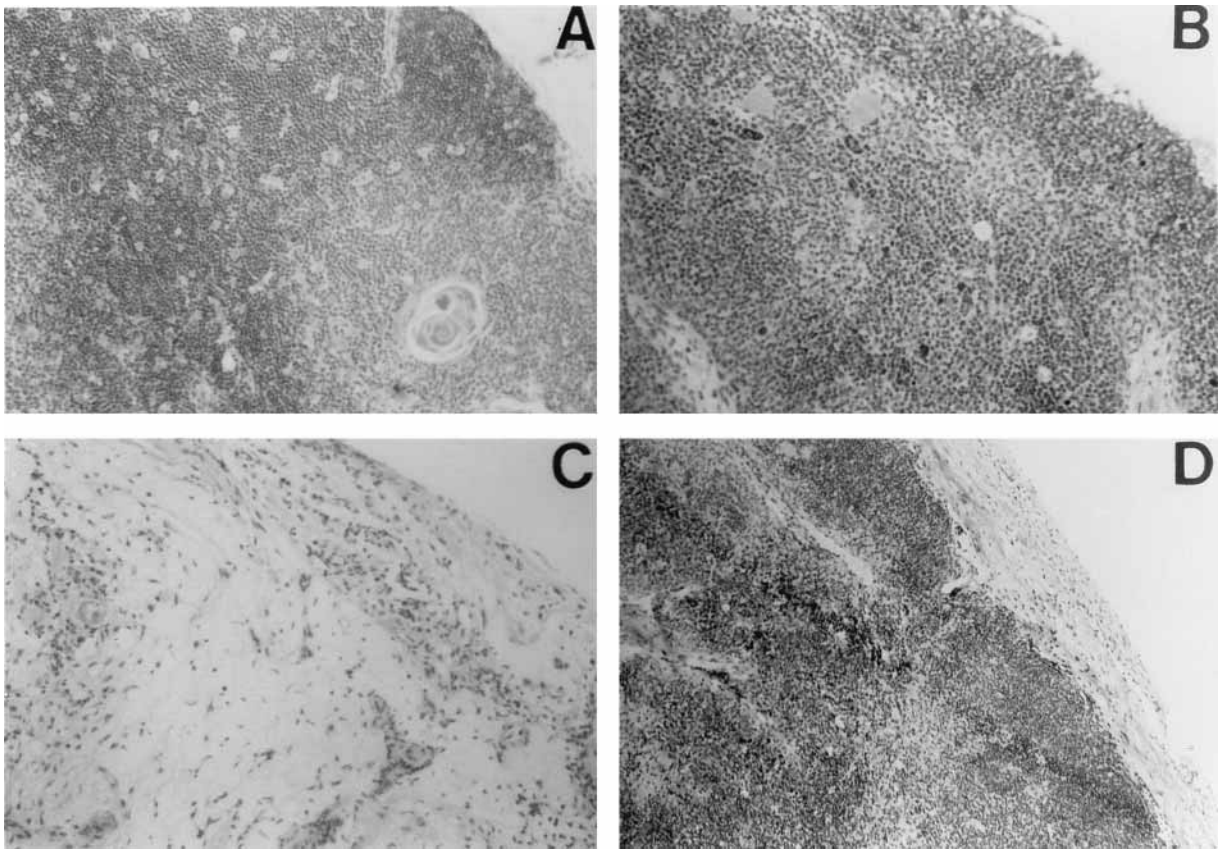

FIG. 3. MV effects on the thymic microenvironment examined from hematoxylin- and eosin-stained sections of paraffin-embedded Thy-Liv implants. (A) Mock-infected Thy-Liv implant, showing thymocytes in densely packed cortices and less densely populated medullas and Hassall's corpuscles. (B) Thy-Liv implant 14 days after infection with Mor, showing maintenance of normal architecture. (C) Thy-Liv implant 14 days following Chi-1 inoculation, showing complete loss of thymocytes. (D) Thy-Liv implant 35 days following Mor infection, demonstrating an intact microenvironment. Magnification, ×400.

CD2 and an increase in the number of cells showing propidium iodide staining, indicating that these thymuses contain fewer viable thymocytes. This population of $CD4^{lo}$ $CD8^{lo}$ cells (Fig. 4C) appears to be composed primarily of dead and dying cells not excluded by gating rather than true $CD4^-$ $CD8^-$ double-negative thymocytes. There was a small decrease in the percentage of $CD4^+$ $CD8^+$ thymocytes after Mor infection with increases in single-positive thymocytes, but $CD2^+$ and propidium iodide-positive cell percentages remained similar to those of mock-infected implants through day 35 (Table 1).

Six SCID-hu implants infected with a different wild-type strain, Bilthoven, (originally isolated and then propagated on human cells) produced thymocyte losses at 7 and 14 days similar to those of Chi-1-infected implants. This suggests that thymic changes due to wild-type viruses are not a result of passage on nonhuman cell lines or unique to the Chi-1 strain.

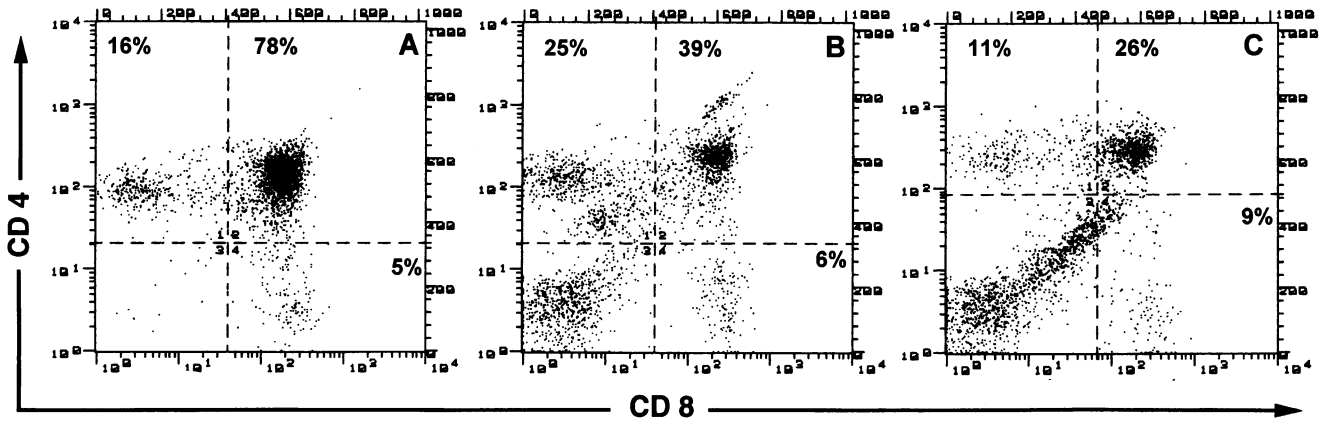

FIG. 4. Representative flow-cytometric analyses of thymocyte subpopulations following wild-type Chi-1 MV infection. Thymocytes were analyzed for expression of CD4 and CD8. (A) Mock-infected implant. Thymocytes from Thy-Liv implants 7 days (B) and 10 days (C) following Chi-1 infection are shown.

Cellular localization of MV replication. To determine if productive MV infection was responsible for the decrease in thymocyte number, thymocytes were stained for the MV viral envelope glycoprotein HA, which is present on cells undergoing active viral replication (18), and for the MV receptor CD46 (membrane cofactor protein) (35), which is downregulated during productive infection with many MV strains (36, 42). There was no evidence of thymocyte expression of MV HA or downregulation of CD46 during infection with either Chi-1 or Mor by flow cytometric analysis. This was true of both dead and dying as well as live cells (data not shown). Therefore, there was no evidence of productive MV infection in thymocytes.

Immunofluorescent colocalization (Fig. 5) on sections from MV-infected Thy-Liv implants was used to identify the cells replicating MV. Extensive MV HA expression was found in thymic epithelial stromal cells expressing human cytokeratins (Fig. 5c) as well as in cells expressing $CD15^+$, a myelomonocytic marker (Fig. 5f). No colocalization of MV HA was seen with antibodies to T-cell markers CD1a, CD2, CD4, or CD45. Immunofluorescent staining with nucleoprotein-specific monoclonal antibody showed a pattern similar to that observed with the HA-specific antibody (data not shown). This mimics the known in vivo tropisms of MV for monocytes and epithelial cells (14, 37). MV HA was present throughout the epithelial stromata in both thymic cortexes and medullas by day 10 during Chi-1 infection, while the distribution was patchy with Mor infection. When the presence of MV HA was correlated to thymic morphology viewed by phase-contrast microscopy, regions of Chi-1 replication correlated precisely with the areas of thymocyte pyknosis and depletion (data not shown). This suggests that thymic disruption is due to the MV effects of local replication in the thymic epithelia.

Wild-type MV induces thymocyte apoptosis. Apoptotic cell death is characterized by DNA fragmentation without evidence of cell necrosis and represents a normal outcome for most thymocytes in vivo (32). Because thymocytes undergo negative selection while in intimate association with thymic stromal epithelial cells (48), the wild-type Chi-1 strain may induce the depletion of thymocytes by epithelially directed apoptosis. Thymocytes following Chi-1 infection (Fig. 6B to C) display a large shift toward dead and dying cells, suggestive of apoptosis, compared with the pattern of cells in mock-infected implants (Fig. 6A). Additional evidence of thymocyte apoptosis was obtained by TUNEL assay, using a digoxigenin-labeled antibody recognizing dUTP attachment to free 3′ OH ends of DNA (Fig. 6D to F). Chi-1 infection induced significant thymocyte DNA fragmentation by day 4 (not shown), and all thymocytes were apoptotic by day 7 (Fig. 6F). Mor infection was comparable to mock infection at early time points (Fig. 6E), with less than 5% apoptotic cells even late in infection (day 35) when higher viral titers were reached (not shown).

DISCUSSION

The thymus is an important target organ for MV infection, but the role of thymic infection in long-term immune suppression, the cellular localization of MV replication, and the roles of MV-strain-specific effects in thymic disruption have not been defined. Using a SCID-hu thymic implant model, we have shown that MV replicates primarily in epithelial and monocytic cells and that an attenuated virus strain replicates more slowly and induces markedly less cellular disruption. In vitro, MV replicates in a wide variety of human and monkey cells, including thymic epithelial cells (39). In this study in vivo, infection of

TABLE 1. Expression of CD4, CD8, and CD2 and viability assessment by staining with propidium iodide after infection of Thy-Liv implants with MV strains Chi-1 and Mor

Cell type(s)	Mean ± SE from indicated MV-infected or control cells on day postinfection[a]:													
	NA[b]	2		7		14		21		28		35		
	Control ($n = 12$)	Chi-1 ($n = 3$)	Mor ($n = 3$)	Chi-1 ($n = 3$)	Mor ($n = 3$)	Chi-1 ($n = 3$)	Mor ($n = 3$)	Chi-1 ($n = 3$)	Mor ($n = 5$)	Chi-1 ($n = 3$)[c]	Mor ($n = 3$)	Mor ($n = 3$)
$CD4^+$ $CD8^-$	14.6 ± 0.5	9.9[d] ± 1.7	15.9 ± 0.9	17.3 ± 5.4	14.7 ± 1.5	19.1 ± 6.2	8.8 ± 1.6	11.7[d] ± 3	34.5 ± 1.7	0.3 ± 0.1	26.9 ± 2.6	23.7 ± 1.7
$CD4^-$ $CD8^+$	7.0 ± 0.4	51.2[d] ± 5.2	18.5 ± 6.8	12.1 ± 6.7	11.7 ± 2.5	14.4 ± 5.5	10.6 ± 2	10.5 ± 3.1	17.6 ± 1.1	0.7 ± 0.2	13.8 ± 2.1	15.1 ± 1.5
$CD4^+$ $CD8^+$	77.1 ± 0.7	37.1[d] ± 3.6	64.4 ± 7.5	66 ± 14.7	71.3 ± 2.9	4.1[e] ± 3.4	72.4 ± 4.4	33.2 ± 12.5	41.9 ± 0.9	0.1 ± 0.1	57.4 ± 4.8	53.4 ± 3.8
$CD4^-$ $CD8^-$	1.1 ± 0.2	1.8 ± 0.3	1.1 ± 0.1	4.7 ± 2.6	2.0 ± 0.6	62.2[d] ± 8	8.2 ± 1.5	35.5 ± 18.6	6.1 ± 3.2	98.9 ± 0.3	1.7 ± 0.1	7.3 ± 4.1
$CD2^+$	99.4 ± 0.1	99.8 ± 0.0	99.7 ± 0.1	97.6 ± 0.6	98.8 ± 0.4	77.1[e] ± 3.4	98.6 ± 0.2	60.6[d] ± 10	98.8 ± 0.2	1.6 ± 0.9	98.7 ± 0.3	98.8 ± 0.6
Propidium iodide positive	2.7 ± 0.6	1.8 ± 0.1	3.1 ± 1.0	6.9 ± 2.2	2.3 ± 0.8	18[d] ± 2.3	0.9 ± 0.5	21.4 ± 10	8.9 ± 1.6	77.8 ± 9.1	4.5 ± 0.5	3.7 ± 0.8

[a] The data represent means of percentages of the specified cell populations or of cells that stained with propidium iodide ± standard errors of these percentages.
[b] NA, not applicable.
[c] $P < 0.0001$.
[d] $P < 0.05$.
[e] $P < 0.001$.

FIG. 5. Immunofluorescent colocalization of MV HA and cellular antigens in Thy-Liv implants 7 days after inoculation with Chi-1. Shown is a photomicrograph following staining to detect MV HA antigen (FITC) (a), human cytokeratin (Texas Red-labeled secondary antibody) (b), MV HA antigen and human cytokeratin (which show the colocalization of MV to thymic epithelia with the characteristic reticular pattern of the stromata surrounding unstained thymocytes) (c), CD15 (FITC), a myelomonocytic marker (d), MV HA antigen (Texas Red-labeled secondary antibody) (e), and CD15 and MV HA (showing colocalization to myelomonocytic cells) (f). Magnification, ×640.

thymic epithelial cells with wild-type MV, but not the attenuated vaccine strain, is associated with thymocyte depletion.

Infection with virulent MV caused complete thymocyte loss in SCID-hu mice and did so without productive infection of thymocytes. Wild-type MV induces apoptosis in Vero cells and a monocytic cell line in vitro (15). Here we show that the apoptotic depletion of thymocytes by wild-type MV is mediated indirectly by infections of thymic epithelial stromata, causing disruption of the thymic microenvironment that normally supports and aids in the selection of immature T cells. SCID-hu mice have also been instructive for the study of HIV (2, 9, 27, 33, 45), CMV (29), and varicella-zoster virus (31), and researchers using these mice have been able to discriminate between syncytium-inducing and nonsyncytial HIV isolates (22). HIV and varicella-zoster virus induce depletion of $CD4^+$ thymocytes (2, 9, 31), but CMV does not (29). Proposed mechanisms of HIV-related thymocyte depletion include direct infection of $CD4^+$ cells and precursors, causing apoptosis (9, 22), indirect mechanisms of thymocyte depletion (46), and disruption of the thymic epithelia (45, 46). Attenuated MV strains such as Mor appear to behave more like CMV (29), which replicates primarily in thymic epithelial cells without having a significant effect on the thymocytes. Well-recognized inducers of thymocyte apoptosis include radiation (43), glucocorticoids (13), cross-linking of the T-cell receptor (44), and growth factor withdrawal (8). Viral infection and thymocyte death have also been described with bovine herpesvirus I (17), chicken anemia virus (21), mouse thymus virus (4), and infectious bursal disease virus (20). However, most of these viruses appear to directly infect thymocytes. Therefore, wild-type MV appears to be the first infection which mediates thymocyte apoptosis wholly by infection of thymic epithelia rather than by thymocyte infection. Potential mechanisms may include a death signal or thymus-specific hormonal withdrawal from MV-infected epithelial cells.

Clinical MV infection generally induces a profound leukopenia that is mainly a T-cell lymphopenia with little change in the peripheral CD4:CD8 ratio (3). MV infection of thymuses has been noted for both humans and primates (23, 30, 38, 40, 52); however, how routinely the virus affects thymuses during measles is not known. Thymic effects alone cannot account entirely for the lymphopenia. MV effects on thymuses and peripheral T-cell populations may be enhanced by the effects of MV on the repertoire of T-cell receptor V_β chains, resulting in long-term alterations in T-cell responses (5). The effects of acute thymocyte loss may be of particular importance for the maturing immune systems of infants and young children who are responding to many new antigenic challenges. Therefore, part of the long-term immune suppression seen with MV infection may be due to infection of thymic epithelial stromata with subsequent loss of thymocytes, thereby affecting subsequent development and function of the peripheral T-cell compartment.

The SCID-hu mouse model is the first small animal model which discriminates virulent from avirulent strains of MV. Since little is known concerning the virulence factors of MV,

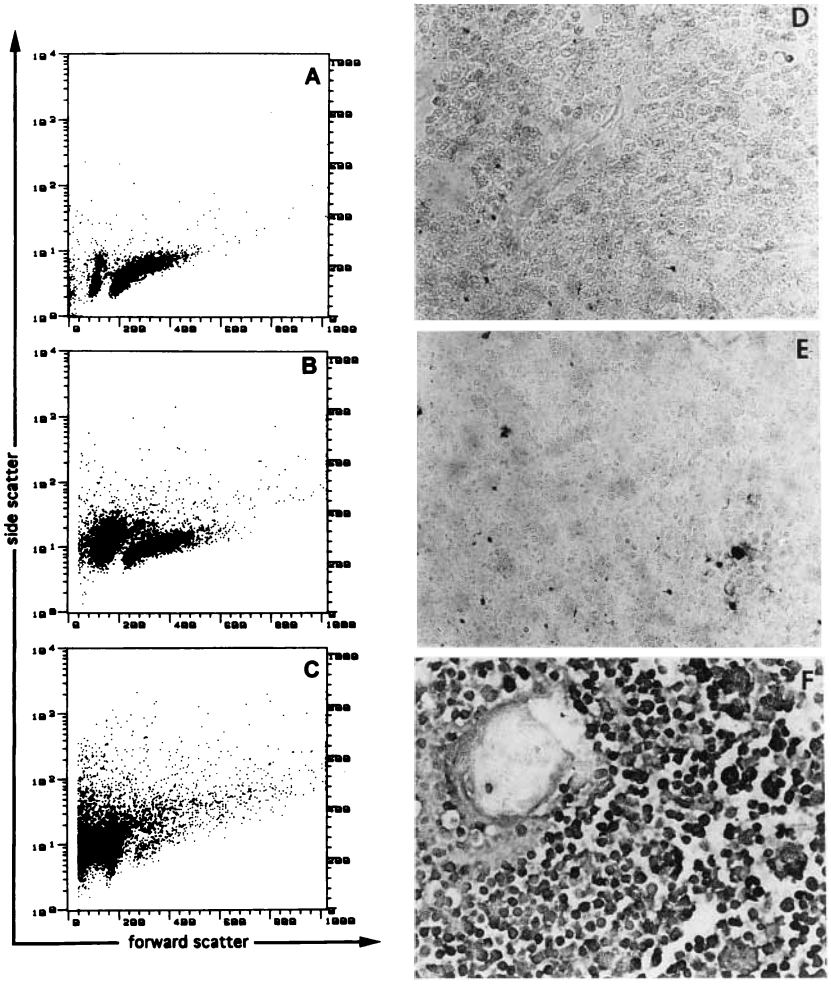

FIG. 6. Analysis by flow cytometry and TUNEL assay of thymocyte cell death following Chi-1 and Mor infection. Flow cytometric analyses of ungated thymocytes are shown with mock-infected cells (A) and with thymocytes 7 days (B) and 14 days (C) following Chi-1 infection. TUNEL assays of paraformaldehyde-fixed sections from Thy-Liv implants are shown with mock-infected cells (D) and with implants 7 days following Mor infection (E) and 7 days following Chi-1 infection (F). Darkly stained cells contain extensive DNA fragmentation suggestive of apoptosis. Magnification, ×525 by phase-contrast microscopy.

SCID-hu mice may provide an experimental model for the study of MV pathogenesis and potentially for testing future live-attenuated vaccines.

ACKNOWLEDGMENTS

This work was supported by Public Health Service grants AI23047 (to D.E.G.) and T32NS07000 (to P.G.A.).

We thank S. Salimi for technical instruction and the staff of the Animal Production Group (SyStemix) for expert implantation of human tissues into SCID mice.

REFERENCES

1. **Albrecht, P., K. Hermann, and G. R. Burns.** 1981. Role of virus strain in conventional and enhanced measles plaque neutralization test. J. Virol. Methods **3:**251–260.
2. **Aldrovandi, G., G. Feuer, L. Gao, B. Jamieson, M. Kristeva, I. S. Y. Chen, and J. A. Zack.** 1993. The SCID-hu mouse as a model for HIV-1 infection. Nature (London) **363:**732–736.
3. **Arneborn, P., and G. Biberfeld.** 1983. T-lymphocyte subpopulations in relation to immunosuppression in measles and varicella. Infect. Immun. **39:**29–37.
4. **Athanassious, R., M. Brunet, and G. Lussier.** 1993. Ultrastructural study of mouse thymus virus replication. Acta Virol. **37:**175–180.
5. **Auwaerter, P. G., G. Hussey, E. Goddard, J. Hughes, J. Ryon, P. Strebel, D. Beatty, and D. E. Griffin.** 1996. Changes within T cell receptor V_β subsets in infants following measles vaccination. Clin. Immunol. Immunopathol. **79:**163–170.
6. **Axton, J. H. M.** 1979. Measles and the state of nutrition. S. Afr. Med. J. **55:**125–126.
7. **Beckford, A. P., R. O. C. Kashula, and C. Stephen.** 1985. Factors associated with fatal cases of measles: a retrospective autopsy study. S. Afr. Med. J. **68:**858–863.
8. **Bhatia, S. K., L. T. Tygrett, K. H. Grabstein, and T. J. Waldschmidt.** 1995. The effect of in vivo IL-7 deprivation on T cell maturation. J. Exp. Med. **181:**1399–1409.
9. **Bonyhadi, M., L. Rabin, S. Salimi, D. A. Brown, J. Kosek, J. M. McCune, and H. Kaneshima.** 1993. HIV induces thymus depletion *in vivo*. Nature (London) **363:**728–732.
10. **Boyd, R. G., and J. F. Boyd.** 1973. The effect of measles on the thymus and other lymphoid tissues. Clin. Exp. Immunol. **13:**343–357.
11. **Bunting, C. H.** 1950. The giant cells of measles. Yale J. Biol. Med. **22:**513–557.
12. **Chino, F., H. Kodama, T. Ohkawa, and Y. Egashira.** 1979. Alterations of the thymus and peripheral lymphoid tissue in fatal measles. Acta Pathol. Jpn. **29:**493–507.
13. **Cohen, J. J.** 1992. Glucocorticoid-induced apoptosis in the thymus. Semin. Immunol. **4:**363–369.
14. **Esolen, L., B. J. Ward, T. R. Moench, and D. E. Griffin.** 1993. Infection of monocytes during measles. J. Infect. Dis. **168:**47–52.
15. **Esolen, L. E., S. W. Park, J. M. Hardwick, and D. E. Griffin.** 1995. Apoptosis as a cause of death in measles virus-infected cells. J. Virol. **69:**3955–3958.
16. **Gavrieli, Y., Y. Sherman, and S. A. Ben-Sasson.** 1992. Identification of programmed cell death in situ via specific labeling of nuclear DNA fragmentation. J. Cell Biol. **119:**493–501.

17. **Griebel, P. J., H. Bielefeldt, M. J. P. Lawman, and L. A. Babiuk.** 1990. The interaction between bovine herpesvirus type 1 and activated bovine T lymphocytes. J. Gen. Virol. **71:**369–377.
18. **Hardwick, J. M., and R. H. Bussell.** 1978. Glycoproteins of measles virus under reducing and nonreducing conditions. J. Virol. **25:**687–692.
19. **Henderson, R. H., J. Keja, G. Hayden, A. Galazka, J. Clements, and C. Chan.** 1988. Immunizing the children of the world: progress and prospects. Bull. W. H. O. **66:**535–543.
20. **Inoue, M., M. Fukada, and K. Miyano.** 1994. Thymic lesions in chicken infected with infectious bursal disease virus. Avian Dis. **38:**839–846.
21. **Jeurissen, S. H., F. Wagenaar, J. M. A. Pol, A. J. van der Eb, and M. H. Notevorn.** 1992. Chicken anemia virus causes apoptosis of thymocytes after in vivo infection and of cell lines after in vitro infection. J. Virol. **66:**7383–7388.
22. **Kaneshima, H., L. Su, M. Bonyhadi, R. I. Connor, D. D. Ho, and J. M. McCune.** 1994. Rapid high, syncytium-inducing isolates of human immunodeficiency virus type 1 induce cytopathicity in the human thymus of the SCID-hu mouse. J. Virol. **68:**8188–8192.
23. **Kobune, F., H. Sakata, and A. Suigiura.** 1990. Marmoset lymphoblastoid cells as a sensitive host for isolation of measles virus. J. Virol. **64:**700–705.
24. **Krowka, J., S. Sarin, R. Namikawa, J. M. McCune, and H. Kaneshima.** 1991. Human T cells in the SCID-hu mouse are phenotypically normal and functionally competent. J. Immunol. **146:**3751–3756.
25. **Liebert, U., and D. Finke.** 1995. Measles virus infection in rodents. Curr. Top. Microbiol. Immunol. **191:**149–166.
26. **McCune, J. M., R. Namikawa, H. Kaneshima, L. D. Shultz, M. Lieberman, and I. L. Weissman.** 1988. The SCID-hu mouse: a model for the analysis of human hematolymphoid differentiation and function. Science **241:**1632–1639.
27. **McCune, J. M., R. Namikawa, C. C. Shih, L. Rabin, and H. Kaneshima.** 1990. Suppression of HIV infection in AZT-treated SCID-hu mice. Science **247:**564–566.
28. **Miller, D. L.** 1963. The frequency of complications of measles. Br. Med. J. **2:**75–78.
29. **Mocarski, E., M. Bonyhadi, S. Salimi, J. M. McCune, and H. Kaneshima.** 1993. Human cytomegalovirus in a SCID-hu mouse: thymic epithelial cells are prominent targets of viral replication. Proc. Natl. Acad. Sci. USA **90:**104–108.
30. **Moench, T. R., D. E. Griffin, C. Obriecht, A. Vaisberg, and R. T. Johnson.** 1988. Acute measles in patients with and without neurological involvement: distribution of measles virus antigen and RNA. J. Infect. Dis. **158:**433–437.
31. **Moffat, J. F., M. D. Stein, H. Kaneshima, and A. M. Arvin.** 1995. Tropism of varicella-zoster virus for human $CD4^+$ and $CD8^+$ T lymphocytes and epidermal cells in SCID-hu mice. J. Virol. **69:**5236–5242.
32. **Murphy, K. M., A. B. Heimberger, and D. Y. Loh.** 1990. Induction by antigen of intrathymic apoptosis of CD4+CD8+TCRlo thymocytes in vivo. Science **250:**1720–1723.
33. **Namikawa, R., H. Kaneshima, M. Lieberman, I. L. Weissman, and J. M. McCune.** 1988. Infection of the SCID-hu mouse by HIV-1. Science **242:** 1684–1686.
34. **Namikawa, R., K. N. Weilbaecher, H. Kaneshima, E. J. Yee, and J. M. McCune.** 1990. Long-term human hematopoiesis in the SCID-hu mouse. J. Exp. Med. **172:**1055–1063.
35. **Naniche, D., G. Varior-Krishnan, F. Cervoni, T. F. Wild, C. Rabourdin-Combe, and D. Gerlier.** 1993. Human membrane cofactor protein (CD46) acts as a cellular receptor for measles virus. J. Virol. **67:**6025–6032.
36. **Naniche, D., T. F. Wild, C. Rabourdin-Combe, and D. Gerlier.** 1993. Measles virus haemagglutinin induces down-regulation of gp57/67, a molecule involved in virus binding. J. Gen. Virol. **74:**1073–1079.
37. **Nii, S., and J. Kamahora.** 1964. Experimental pathology of measles in monkeys. Biken J. **6:**271–297.
38. **Nozawa, Y., N. Ono, M. Abe, H. Sakuma, and H. Wakasa.** 1994. An immunohistochemical study of Warthlin-Finkeldey cells in measles. Pathol. Int. **44:**442–447.
39. **Numazaki, K., H. Goldman, I. Wong, and M. A. Wainberg.** 1989. Replication of measles virus in cultured human thymic epithelial cells. J. Med. Virol. **27:**52–58.
40. **Sakaguchi, M., Y. Yoshikawa, K. Yamanouchi, T. Sata, K. Nagashima, and K. Takeda.** 1986. Growth of measles virus in epithelial and lymphoid tissue of cynomolgus monkeys. Microbiol. Immunol. **30:**1067–1073.
41. **Samse, T. K., T. Ruspandji, I. Susanto, and K. Gunawan.** 1994. Risk factors for severe measles. Southeast Asian J. Trop. Med. Public Health **23:**491–503.
42. **Schneider-Schaulies, J., L. M. Dunster, F. Kobune, B. Rima, and V. ter Meulen.** 1995. Differential downregulation of CD46 by measles virus strains. J. Virol. **69:**7257–7259.
43. **Sellins, K. S., and J. J. Cohen.** 1987. Gene induction by γ-irradiation leads to DNA fragmentation in lymphocytes. J. Immunol. **139:**3199–3206.
44. **Smith, C. A., G. T. Williams, R. Kingston, E. J. Jenkinson, and J. J. T. Owen.** 1989. Antibodies to CD3/TCR complex induce death by apoptosis in immature T cells in thymic culture. Nature (London) **337:**181–183.
45. **Stanley, S. K., J. M. McCune, H. Kaneshima, J. S. Justement, M. Sullivan, E. Boone, M. Baseler, J. Adelsberger, M. Bonyhadi, J. Orenstein, C. H. Fox, and A. S. Fauci.** 1993. Human immunodeficiency virus infection of the human thymus and disruption of the human thymic microenvironment in the SCID-hu mouse. J. Exp. Med. **178:**1151–1163.
46. **Su, L., H. Kaneshima, M. Bonyhadi, S. Salimi, D. Kraft, L. Rabin, and J. M. McCune.** 1995. HIV-1 induced thymocyte depletion is associated with indirect cytopathicity and infection of progenitor cells in vivo. Immunity **2:**25–36.
47. **van Binnendijk, R., R. van der Heijden, and A. D. M. E. Osterhaus.** 1995. Monkeys in measles research. Curr. Top. Microbiol. Immunol. **191:**135–148.
48. **van Ewijk, W.** 1991. T cell differentiation is influenced by thymic microenvironments. Annu. Rev. Immunol. **9:**591–615.
49. **von Pirquet, C.** 1908. Verhalten der Kuten tuberkulin-Reaktion wahrend der Masern. Dtsch. Med. Wochenschr. **34:**1297–1300.
50. **Ward, B. J., and D. E. Griffin.** 1993. Differential CD4 T cell activation in measles. J. Infect. Dis. **168:**275–281.
51. **Ward, B. J., R. T. Johnson, A. Vaisberg, A. Jauregui, and D. E. Griffin.** 1990. Cytokine production in vitro and the lymphoproliferative defect of natural measles virus infection. Clin. Immunol. Immunopathol. **55:**315–326.
52. **Yamanouchi, K., F. Chino, F. Kobune, H. Kodama, and T. Tsuruhara.** 1973. Growth of measles virus in the lymphoid tissue of monkeys. J. Infect. Dis. **128:**795–799.

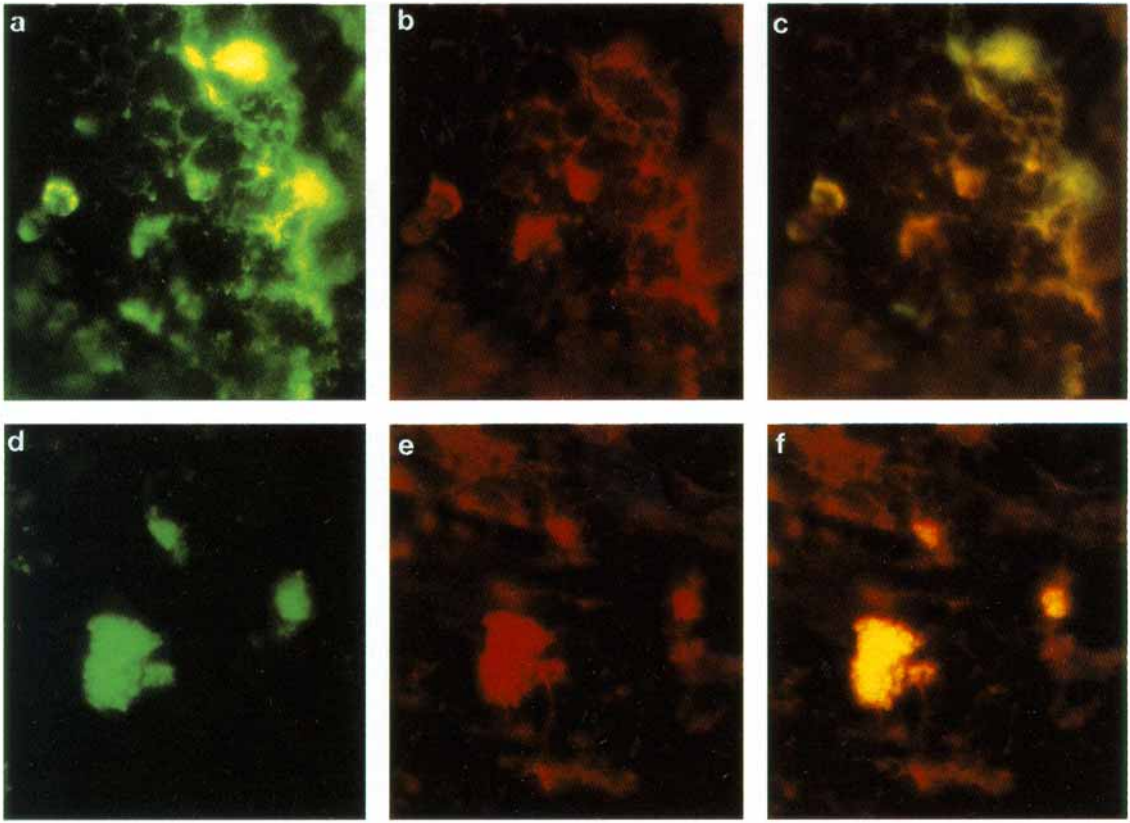
a
b
c
d
e
f